

# Calculating Combined Buoyancy- and Pressure-driven Flow Through a Shallow, Horizontal, Circular Vent: Application to a Problem of Steady Burning in a Ceiling-vented Enclosure

L. Y. Cooper

Building and Fire Research Laboratory, National Institute of Standards and Technology,  
Gaithersburg, MD 20899, USA

(Received 21 September 1995; revised version received 5 March 1996;  
accepted 20 May 1996)

## ABSTRACT

*A model was developed previously for calculating combined buoyancy- and pressure-driven (i.e. forced) flow through a shallow, circular, horizontal vent where the vent-connected spaces are filled with fluids of different density in an unstable configuration (density of the top fluid is larger than that of the bottom). In this paper the model is summarized and then applied to the problem of steady burning in a ceiling-vented enclosure where normal atmospheric conditions characterize the upper-space environment. Such fire scenarios are seen to involve a zero to relatively moderate cross-vent pressure difference and bidirectional exchange flow between the enclosure and the upper space. A solution to the problem leads to a general result that relates the rate of energy release of the fire to the area of the vent and the temperature and oxygen concentration of the upper portion of the enclosure environment. This result is seen to be consistent with previously published data from experiments involving ceiling-vented fire scenarios. Published by Elsevier Science Ltd.*

## NOTATION

$A_v$	Vent area
$C_{O_2}$	Eqn (15)
$c_{LOW, O_2}, c_{LOW, CO_2}$	Molal fractions of $O_2$ , $CO_2$ in lower part of enclosure
$D$	Diameter of vent or burner
$g$	Acceleration of gravity

$H$	Characteristic elevation interval of the flow problem
$L$	Depth of vent
$M$	9.400 in eqn (11), or mass of fuel
$p; p_{\text{HIGH}}, p_{\text{LOW}}$	Pressure; far-field $p$ on high-, low-pressure side of vent, near the vent elevation
$\bar{p}$	$(p_{\text{HIGH}} + p_{\text{LOW}})/2$
$\dot{Q}; \dot{Q}_{\text{MEAS}}; \dot{Q}_{\text{MAX}}$	Burning rate; measured in Jansson <i>et al.</i> ; <sup>11</sup> maximum of $\dot{Q}$
$\dot{Q}^*$	Dimensionless, eqn (16)
$R$	Gas constant
$T; T_{\text{TOP}}, T_{\text{BOT}}; T_{\text{AMB}}; T^*$	Absolute temperature; far field $T$ in top, bottom space, near the vent elevation; $T$ of ambient; $T/T_{\text{AMB}}$
$T_{\text{UP, AVE}}$	Average of upper-enclosure $T$ measured in Jansson <i>et al.</i> <sup>11</sup>
$\bar{T}$	$(T_{\text{TOP}} + T_{\text{BOT}})/2$
$\dot{V}_{\text{EX, MAX}}$	Maximum exchange flow rate, at $\Delta p = 0$ , i.e. maximum possible $\dot{V}_{\text{LOW}}$
$\dot{V}_{\text{FLOOD}}$	$\dot{V}_{\text{HIGH}}$ at onset of flooding
$\dot{V}_{\text{HIGH}}, \dot{V}_{\text{LOW}}$	Volumetric flow rates from high- to low-pressure and from low- to high-pressure side of vent
$\dot{V}_{\text{TOP}}, \dot{V}_{\text{BOT}}$	Volumetric flow rates from top to bottom side and from bottom to top-side of vent
$\dot{V}_{\text{NET}}$	$\dot{V}_{\text{HIGH}} - \dot{V}_{\text{LOW}}$

### Greek symbols

$\Delta p, \Delta p_{\text{FLOOD}}$	$p_{\text{HIGH}} - p_{\text{LOW}}; \Delta p$ at onset of flooding
$\Delta \rho$	$\rho_{\text{TOP}} - \rho_{\text{BOT}}$
$\delta p^*$	$\Delta p / \Delta p_{\text{FLOOD}}$
$\epsilon'$	Dimensionless $\Delta \rho$ , eqn (9)
$\lambda$	Eqn (11)
$\rho; \rho_{\text{TOP}}, \rho_{\text{BOT}}$	Density; far-field $\rho$ in top, bottom space, near the vent elevation
$\phi$	Eqns (10) and (11)
$\psi; \psi_{\text{AMB}}; \psi_{\text{LOW}}$	Mass concentration of $\text{O}_2$ in: the upper part of enclosure; the ambient; and the lower part of enclosure
$\psi_{\text{EXT}}$	$\psi_{\text{LOW}}$ at extinction

## 1 INTRODUCTION

Consider the flow through a horizontal vent (i.e. a vent or hole in a horizontal partition) where the fluids which fill the vent-connected spaces near the elevation of the vent are of different density and in an unstable configuration, a relatively dense fluid in the upper space,  $\rho_{TOP}$ , overlaying a relatively less dense fluid in the lower space,  $\rho_{BOT}$ :

$$\Delta\rho = \rho_{TOP} - \rho_{BOT} > 0 \quad (1)$$

Consider the cross-vent pressure difference, as would be measured near the elevation of the vent, but removed laterally from the effects of possible through-vent flows. If the pressure above the vent in the upper space is significantly greater than the pressure below the vent in the lower space, then there will be a downward, unidirectional, orifice-type flow of the relatively dense fluid through the vent, from the top space to the bottom space. Similarly, if the pressure below is significantly greater than above, then the flow will again be unidirectional, with the relatively less dense fluid flowing upward from the bottom to the top space.

If the pressure drop across the vent is exactly zero then in theory the configuration of more dense over less dense fluid can exist in an equilibrium state, i.e. with no flow at all. However, the latter equilibrium state is unstable in the sense that any small perturbations of the horizontal interface that separates the fluids will grow in amplitude, become larger, and eventually lead to an exchange flow across the vent, with the relatively dense fluid dropping down through part of the vent area and the relatively less dense fluid rising upwards through the rest of the vent area. The zero-pressure drop case is illustrated by a simple experiment involving the emptying from the bottom of a liquid-filled can with a single vent opening or of a liquid-filled bottle. In both cases a thin sheet of plastic across the opening can maintain the system in a zero-flow equilibrium state (i.e. there is zero pressure drop across the interface). However, the hydrostatic system is unstable, and removal of the plastic sheet leads immediately to emptying of the vessel by means of simultaneous, cross-vent exchanges of liquid from above and air from below.

As the cross-vent pressure difference goes from zero to significant values, the rates of flow from the high- and low-pressure sides of the vent increase and decrease, respectively, until the precise point where unidirectional flow is initiated. The latter condition will be referred to below as the flooding flow condition.

The interested reader is referred to the work of Cooper<sup>1</sup> for a more

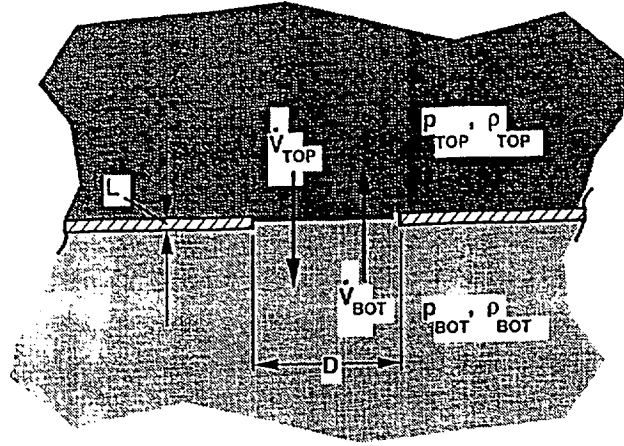


Fig. 1. The basic horizontal vent configuration.

detailed discussion of the above phenomena, including references to the relevant literature.

The focus of this work is on problems where the fluids in the upper and lower spaces can both be accurately described as the same perfect gas in the sense that use of identical gas-property models in the two spaces would lead everywhere to accurate estimates of thermodynamic and transport properties. Relative to the technology of fire safety, a prototype example of such problems involves flows through a vent where uncontaminated ambient-temperature air in an upper space overlays elevated-temperature combustion product-contaminated or 'smokey' air in a lower space.

Assume that in each space, laterally removed from the vent, the environment is relatively quiescent with pressure well-approximated by the hydrostatic pressure field. As in Fig. 1, designate the spaces connected by the vent as top and bottom. Subscripts TOP and BOT, respectively, refer to conditions in these spaces near the vent elevation, but removed laterally from the vent. Similarly, subscripts HIGH and LOW refer to the conditions on the high- and low-pressure sides of the vent, respectively.

$\dot{V}_{TOP}$  and  $\dot{V}_{BOT}$  are the volume flow rates through the vent from the top to the bottom side of the vent and from the bottom to the top side of the vent, respectively. Similarly,  $\dot{V}_{HIGH}$  and  $\dot{V}_{LOW}$  are the volume flow rates from the high- to the low-pressure side and from the low- to the high-pressure side of the vent. Flow through the vent is determined by: the design of the vent, its shape and its depth,  $L$ ;  $\rho_{TOP}$  and  $\rho_{BOT}$ ; and the pressures,  $p_{TOP}$  and  $p_{BOT}$ .

The cross-vent pressure difference is

$$\begin{aligned} \Delta p = p_{HIGH} - p_{LOW} \geq 0, \quad p_{HIGH} = \max(p_{TOP}, p_{BOT}), \\ p_{LOW} = \min(p_{TOP}, p_{BOT}) \end{aligned} \quad (2)$$

$\Delta p$  and the characteristic elevation interval of the flow problem,  $H$  (e.g. the combined height of the two spaces joined by the vent of interest), are assumed to be so small that

$$\Delta \rho g |H| / \bar{p} \ll 1, \quad \Delta p / \bar{p} \ll 1, \quad \bar{p} = (p_{\text{HIGH}} + p_{\text{LOW}}) / 2 \quad (3)$$

where  $g$  is the acceleration of gravity. Then, for the purpose of establishing the interdependence throughout the flow region of density,  $\rho$ , and temperature,  $T$ , the equation of state for the gas can be well approximated by

$$\rho T = \text{constant} = \rho_{\text{TOP}} T_{\text{TOP}} = \rho_{\text{BOT}} T_{\text{BOT}} = \bar{p} / R \quad (4)$$

where  $R$  is the gas constant and temperatures  $T_{\text{TOP}}$  and  $T_{\text{BOT}}$  correspond to specified  $\rho_{\text{TOP}}$  and  $\rho_{\text{BOT}}$  in eqn (4).

For any unstable arrangement of densities across a vent there will always be a value  $\Delta p = \Delta p_{\text{FLOOD}}$ , denoted as the critical or flooding value of  $\Delta p$ , which separates a unidirectional or 'flooding' flow regime ( $\Delta p \geq \Delta p_{\text{FLOOD}}$ ) where  $\dot{V}_{\text{LOW}} = 0$ , from a 'mixed' flow regime ( $0 \leq \Delta p < \Delta p_{\text{FLOOD}}$ ) where  $\dot{V}_{\text{LOW}} > 0$ . Associated with any particular  $\Delta p_{\text{FLOOD}}$  value is a corresponding volumetric flooding flow rate,  $\dot{V}_{\text{FLOOD}} = \dot{V}_{\text{HIGH}}(\Delta p = \Delta p_{\text{FLOOD}})$ . When  $\Delta p = 0$ ,  $\dot{V}_{\text{HIGH}} = \dot{V}_{\text{LOW}}$  and the HIGH/LOW designations are arbitrary.

$\dot{V}_{\text{NET}}$  is the net volume flow rate from the high to the low-pressure side of the vent:

$$\dot{V}_{\text{NET}} = \dot{V}_{\text{HIGH}} - \dot{V}_{\text{LOW}} \geq 0 \quad (5)$$

This is the forced or pressure-driven part of the vent flow. At the two extremes of the mixed flow regime,  $\dot{V}_{\text{NET}} = \dot{V}_{\text{FLOOD}}$  at  $\Delta p = \Delta p_{\text{FLOOD}}$  and  $\dot{V}_{\text{NET}} = 0$  at  $\Delta p = 0$ . Similarly,  $\dot{V}_{\text{LOW}}$  is the buoyancy-driven part of the flow, and a nonzero value for this corresponds to nonzero 'exchange flow'.  $\dot{V}_{\text{LOW}} = 0$  when  $\Delta p = \Delta p_{\text{FLOOD}}$  and  $\dot{V}_{\text{LOW}}$  reaches its maximum value,  $\dot{V}_{\text{EX, MAX}}$ , as  $\Delta p$  and the forced part of the flow go to zero.

## 2 THE ALGORITHM VENTCL2 FOR DETERMINING $\dot{V}_{\text{HIGH}}$ AND $\dot{V}_{\text{LOW}}$ THROUGH A SHALLOW CIRCULAR VENT FOR ARBITRARY VALUES OF $p_{\text{TOP}}$ , $p_{\text{BOT}}$ AND $\rho_{\text{TOP}} > \rho_{\text{BOT}}$

For arbitrary specified values of  $p_{\text{TOP}}$ ,  $p_{\text{BOT}}$  and  $\rho_{\text{TOP}} > \rho_{\text{BOT}}$ , a mathematical model and concise algorithm, VENTCL2, to calculate  $\dot{V}_{\text{HIGH}}$  and  $\dot{V}_{\text{LOW}}$  was developed and presented by Cooper.<sup>1</sup> Use of the model and algorithm is limited to the prediction of turbulent, large Grashof number flows<sup>1</sup>

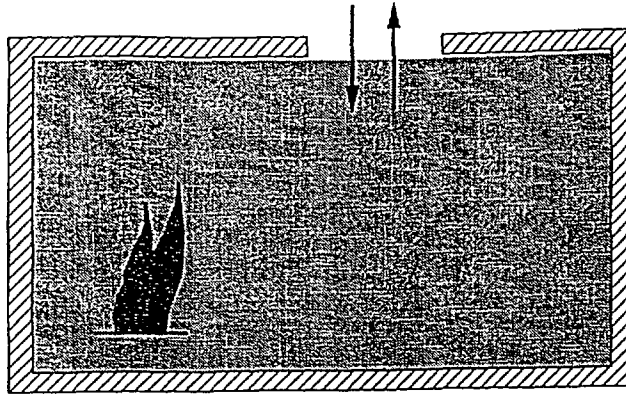


Fig. 2. Configuration of a ceiling vented room with a fire.

through a shallow ( $L/D < 1$ ), circular vents. VENTCL2 is an advanced version of the algorithm VENTCL.<sup>2,3</sup>

### 3 APPLICATIONS OF VENTCL2: STEADY BURNING IN A CEILING-VENTED ROOM

#### 3.1 The problem

Consider a room with a fire, fully enclosed except for a shallow circular ceiling vent. Refer to Fig. 2. The air above the vent has ambient density, absolute temperature and oxygen ( $O_2$ ) mass concentrations of  $\rho_{AMB}$ ,  $T_{AMB}$  and  $\psi_{AMB}$ , respectively. Assume steady conditions where the room environment immediately below the vent has density, temperature and  $O_2$  mass concentrations of  $\rho$ ,  $T > T_{AMB}$  and  $\psi < \psi_{AMB}$ , respectively.  $\psi_{LOW}$ , the  $O_2$  mass concentration in the lower part of the room at the elevation of the fire, must exceed the minimum extinction value,  $\psi_{EXT}$ , associated with the particular fuel. For example, for the combustion of  $CH_4$  diffusion flames from round burners with diameters  $D$  in the range  $0.089 \text{ m} \leq D \leq 0.50 \text{ m}$ ,  $\psi_{EXT}$  was measured in previous works<sup>4,5</sup> as ranging from 0.140 ( $D = 0.50 \text{ m}$ ) to 0.161 ( $D = 0.089 \text{ m}$ ).

The conjectured steady-state condition must involve an exchange flow through the vent, with relatively-dense, ambient-temperature,  $O_2$ -rich air flowing down through the vent from above, and relatively-less-dense, elevated-temperature, product-of-combustion laden,  $O_2$ -lean 'air' flowing up through the vent from below. As the cool ambient air enters the room, it drops downward through the relatively-less-dense room environment as a negatively buoyant plume. As the plume descends, it entrains the elevated temperature,  $O_2$ -lean, room gases, and, as a result, continuously

increases in mass flow rate and temperature and decreases in O<sub>2</sub> concentration. The plume gases, including the convected O<sub>2</sub>, are deposited in the lower part of the room. Compared to the environment in the upper part of the room, the continuously deposited plume flow maintains the environment of the lower part of the room in a relatively cool and relatively-O<sub>2</sub>-rich state (i.e.  $\psi_{\text{LOW}} > \psi$ ). It is the latter environment that engulfs the fire and supplies it with the O<sub>2</sub> required to maintain its combustion processes.

In the next two sections, the VENTCL2 algorithm will be used to estimate the exchange flow through the vent and the burning rate that can be supported by the net rate of oxygen inflow for specified values of  $\rho$ ,  $T$  and  $\psi$ .

### 3.2 The relationship between $\delta p$ and $T$

Assume that: the mass flow-rate of fuel introduced by the fire is negligible compared to the mass flow-rates associated with the exchange flow; the environment both inside and outside the room has the thermodynamic properties of air, well approximated by a perfect-gas model; and there is no mixing in the vent, i.e. all inflow is at the ambient condition and all outflow is from the bulk upper room environment. (Note that while the latter assumption on mixing in the vent is reasonable, it is worthy of further study. Such study is beyond the scope of the present work.)

Using the approximation of eqn (3), it follows from eqn (4) that

$$T/T_{\text{AMB}} = \rho_{\text{AMB}}/\rho = \rho_{\text{TOP}}/\rho_{\text{BOT}} > 1 \quad (6)$$

From eqns (1) and (6) it is evident that the present problem involves an unstable configuration. Therefore the VENTCL2 flow algorithm is applicable.

Conservation of mass across the vent requires

$$\rho \dot{V}_{\text{BOT}} = \rho_{\text{AMB}} \dot{V}_{\text{TOP}} \quad (7)$$

Using eqn (6), it follows from eqn (7) that  $\dot{V}_{\text{BOT}} > \dot{V}_{\text{TOP}} > 0$ . Therefore the high- and low-pressure sides of the vent are at the bottom and top, respectively, and the problem involves the mixed-flow regime.

$$\dot{V}_{\text{HIGH}} = \dot{V}_{\text{BOT}}, \quad \dot{V}_{\text{LOW}} = \dot{V}_{\text{TOP}}, \quad \rho_{\text{HIGH}} = \rho, \quad \rho_{\text{LOW}} = \rho_{\text{AMB}} \quad (8)$$

Following VENTCL2,<sup>1</sup> define

$$\begin{aligned} \epsilon' &= -\Delta p/\bar{p} = -2\Delta p/(\rho + \rho_{\text{AMB}}) = -2(T^* - 1)/(T^* + 1) < 0, \\ T^* &\equiv T/T_{\text{AMB}} = (2 - \epsilon')/(2 + \epsilon'), \quad \delta p^* = \Delta p/\Delta p_{\text{FLOOD}}, \\ \Delta p_{\text{FLOOD}} &= 0.2427(4g\Delta\rho D)(1 + \epsilon'/2) \exp(1.1072\epsilon') \end{aligned} \quad (9)$$

Then VENTCL2 is found to require the following dependence of  $\delta p^*$  on  $\epsilon'$ :

$$\phi(\delta p^*) = \lambda(\epsilon') \quad (10)$$

where

$$\lambda(\epsilon') = -2(0.282)\epsilon' \exp(-0.5536\epsilon')/(2 + \epsilon'),$$

$$\phi(\delta p^*) = \{M - [1 + (M^2 - 1)(1 - \delta p^*)]^{1/2}\}$$

$$/ \{ (M + 1)[0.6465(1 - \delta p^*)^2 - 1.6465(1 - \delta p^*)] \}, \quad M = 9.400 \quad (11)$$

Using the numerical root-finder RTSAFE,<sup>6</sup> the solution of eqn (10) for  $\delta p^*$  as a function of  $\epsilon'$  or  $T/T_{AMB}$  was found for a wide range of  $\epsilon' < 0$  ( $T > T_{AMB}$ ). This is plotted in Fig. 3.

### 3.3 The energy release rate of the fire as a function of $T$ and its maximum possible value

The energy-release rate  $\dot{Q}$  of the fire is related to the fraction of  $O_2$  inflow which is consumed by the combustion.

Equations (7) and (8) and the following results from Epstein<sup>7</sup>

$$\dot{V}_{EX, MAX} = 0.055(4/\pi)A_V(gD|\epsilon'|)^{1/2} \quad (12)$$

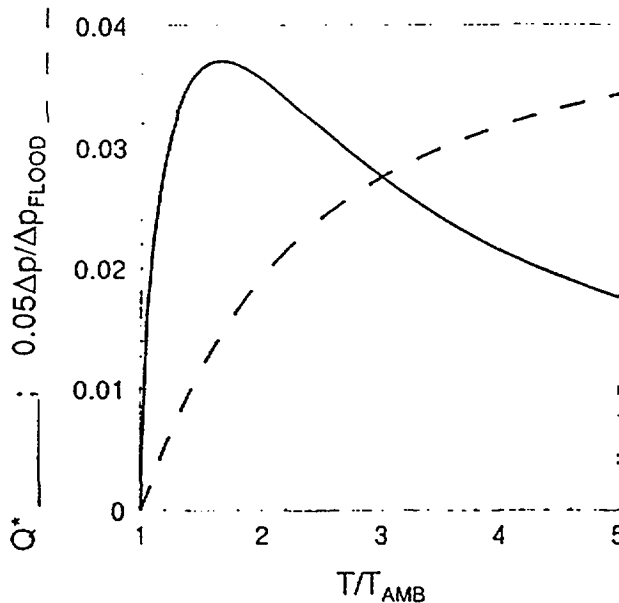


Fig. 3. Plots of  $\Delta p/\Delta p_{FLOOD}$  and  $\dot{Q}^* = / [(1 - \psi/\psi_{AMB})\rho_{AMB}\psi_{AMB}C_{O_2}A_V^{5/2}g^{1/2}]$  as functions of  $T/T_{AMB}$  for the configuration of Fig. 2.

lead to

net rate of O<sub>2</sub> consumption

$$\begin{aligned} &= \psi_{\text{AMB}} \rho_{\text{AMB}} \dot{V}_{\text{LOW}} - \psi \rho_{\text{HIGH}} \dot{V}_{\text{HIGH}} \\ &= 0.055 D^{5/2} g^{1/2} |\epsilon'|^{1/2} \psi_{\text{AMB}} \rho_{\text{AMB}} (1 - \psi/\psi_{\text{AMB}}) \dot{V}_{\text{LOW}}/\dot{V}_{\text{EX, MAX}} \end{aligned} \quad (13)$$

where  $\dot{V}_{\text{LOW}}/\dot{V}_{\text{EX, MAX}}$  as a function of  $\delta p^*$  can be obtained from<sup>1</sup>

$$\dot{V}_{\text{LOW}}/\dot{V}_{\text{EX, MAX}} = [0.6465(1 - \delta p^*)^2 - 1.6465(1 - \delta p^*)]^2 \quad (14)$$

From Huggett:<sup>8</sup>

$$C_{\text{O}_2} \equiv \dot{Q}/(\text{net rate of O}_2 \text{ consumed}) = 13.2 \times 10^3 \text{ kW}/(\text{kg}_{\text{O}_2}/\text{s}) \quad (15)$$

Using eqn (13) in eqn (15) and defining a dimensionless  $\dot{Q}$ ,

$$\dot{Q}^* \equiv \dot{Q}/[(1 - \psi/\psi_{\text{AMB}}) \rho_{\text{AMB}} \psi_{\text{AMB}} C_{\text{O}_2} A^{5/4} v g^{1/2}] \quad (16)$$

leads to

$$\dot{Q}^* = 0.074 |\epsilon'|^{1/2} \dot{V}_{\text{LOW}}/\dot{V}_{\text{EX, MAX}} \quad (17)$$

The previously determined  $\delta p^*$  vs  $\epsilon'$  solutions were used in eqns (11), (14) and (17) to obtain  $\dot{Q}^*$  vs  $T/T_{\text{AMB}}$  and this is plotted in Fig. 3. From this it is seen that  $\dot{Q}^*$  is predicted to rise rapidly from 0, at  $T/T_{\text{AMB}} = 1$ , to a maximum value,  $\dot{Q}_{\text{MAX}}^* = 0.037$ , at  $T/T_{\text{AMB}} = 1.65$ , and to monotonically decrease with further increases of  $T/T_{\text{AMB}}$ . Associated with  $\dot{Q}_{\text{MAX}}^*$ , let  $\dot{Q}_{\text{MAX}}$  be the maximum possible  $\dot{Q}$  for a given  $\psi$ . Taking  $T_{\text{AMB}} = 300 \text{ K}$ ,  $\rho_{\text{AMB}} = 1.2 \text{ kg/m}^3$ ,  $\psi_{\text{AMB}} = (0.23 \text{ kg O}_2)/\text{kg}$ , and  $g = 9.8 \text{ m/s}^2$ , eqns (15) and (16) lead to

$$\dot{Q}_{\text{MAX}} = 0.41(10^3) \{1 - \psi/[0.23(\text{kg O}_2)/\text{kg}]\} (A_v/\text{m}^2)^{5/4} \text{ kW} \quad (18)$$

From eqn (18) it is clear that the scenario leading to the largest value of  $\dot{Q}_{\text{MAX}}$  is one where the concentration of O<sub>2</sub> in the upper part of the room is close to zero, i.e.  $\psi$  is negligible. (This would likely occur when  $\psi_{\text{LOW}} \approx \psi_{\text{EXT}}$ .) Setting  $\psi = 0$  in eqn (18) leads to the upper bound estimate for  $\dot{Q}_{\text{MAX}}$ :

$$\dot{Q}_{\text{MAX}} < 0.41(10^3) (A_v/\text{m}^2)^{5/4} \text{ kW} = 0.41 \times 10^3 \text{ kW}, 1.3 \text{ kW} \text{ and } 0.23 \text{ kW}$$

$$\text{for } A_v = 1.0 \text{ m}^2, 1.0 \times 10^{-2} \text{ m}^2 \text{ and } 25.0 \times 10^{-4} \text{ m}^2, \text{ respectively} \quad (19)$$

The reader is referred to the work of Epstein<sup>9</sup> who uses alternative means to develop an upper-bound estimate for  $\dot{Q}_{\text{MAX}}$ . In this regard, Equation (13) from this past work<sup>9</sup> is equivalent to eqn (19), with 0.41 being replaced by 0.6.

The results of Fig. 3 are now related to data acquired in 'full-scale' experiments reported elsewhere.<sup>10,11</sup> In this it is assumed that the present

circular-vent results can be used to provide estimates for the square- and rectangular-vented enclosures used in the experiments.

### 3.4 Experimental validation of the Fig. 3 solution

#### 3.4.1 Fire in ceiling-vented ship quarters.

The work of Steward *et al.*<sup>10</sup> reports on a fire in a mock-up fully-furnished three-person ship accommodation quarter ( $3.84 \times 2.82 \times 2.38$  m high), fully enclosed except for a single square vent,  $A_v = 1$  m<sup>2</sup>, in a corner of the ceiling, away from the furnishings. The fire involved an initial interval of intense burning which rapidly decayed to smoldering (10 min), an interval of smoldering (20 min), and a final interval of intense burning (30 min). The final interval involved a 19–20 min sub-interval in which the heat release rate was relatively constant at  $\dot{Q} = (0.25 \pm 0.05)10^3$  kW. It is reasonable to expect that the latter sub-interval was a time of steady state during which the present example analysis of ventilation conditions is relevant. Indeed, the measured burn rate does satisfy the criterion of eqn (18), i.e.  $\dot{Q} = (0.25 \pm 0.05) \times 10^3$  kW  $< \dot{Q}_{MAX} < 0.41 \times 10^3$  kW. Also, Fig. 3, eqn (18) and the measured value of  $\dot{Q}$  lead to the estimate  $\psi < 0.09(1 \pm 0.3)$  (kg O<sub>2</sub>)/kg. There is no reported measured value of  $\psi$  to validate the latter estimate. However, the result is plausible since (assuming  $\psi_{EXT} \approx \psi_{EXT}$  for CH<sub>4</sub>), as required, the latter estimated value for  $\psi$  is less than the expected value of  $\psi_{LOW}$ , which would have been in the range  $\psi_{AMB} = 0.23$  (kg O<sub>2</sub>)/kg  $< \psi_{LOW} < \psi_{EXT} \approx 0.15$  (kg O<sub>2</sub>)/kg.

#### 3.4.2 Wood fires in a ceiling-vented 218 m<sup>3</sup> cubic enclosure.

Jansson *et al.*<sup>11</sup> reported on five experiments involving wood fires located at the center of the floor of a cubic room ( $6 \times 6 \times 6$  m), fully enclosed except for a single, centrally located, ceiling vent. Three vents were used:  $A_v = 4$  m<sup>2</sup> ( $2 \times 2$  m),  $2$  m<sup>2</sup> ( $1 \times 2$  m) and  $1$  m<sup>2</sup> ( $1 \times 1$  m). The burn times were 30 min. Measured and reported variables included:  $dM/dt$ , where  $M$  is the mass of the fuel;  $T_{UP, AVE}$ , the average of the upper-enclosure temperatures; and  $c_{LOW, O_2}$ ,  $c_{LOW, CO_2}$ , the molal fractions of O<sub>2</sub> and CO<sub>2</sub>, respectively, in the lower part of the enclosure, 1 m from the floor and 1 m from the combustion zone. The data were studied to identify intervals that could be reasonably construed to represent quasi-steady-state conditions for which the present example calculation would be relevant. The selected criterion for this was that all measured variables reported in the study<sup>11</sup> were relatively constant over an interval of at least 5 min.

The ‘best’ steady-state interval was found and analyzed for experiments 2–4. No steady-state intervals were identified in experiments 1 and 5.

For the experiments, the heat of combustion of the wood fuel was

**TABLE 1**  
Data on Ceiling-Vented Wood Fire Scenarios<sup>11</sup> and Application of Fig. 3 and eqns (15) and (16)

Experiment number, interval, initial mass	$A_V [m^2]$	$T_{UP, AVE} [K]$ <i>measured</i>	$\dot{Q}_{MEAS} [kW]$ <i>measured</i>	$\psi [(kg O_2)/kg]$ <i>calculated</i>	$\psi_{LOW} [(kg O_2)/kg]$ <i>measured</i>
2, 15–20 min, 100 kg	2	440 ± 6	410 ± 40	0.13	0.15
3, 15–20 min, 100 kg	1	386 ± 1	170 ± 7	0.12	0.15
4, 5–10 min, 25 kg	4	373 ± 5	370 ± 60	0.19	0.21

taken to be<sup>12</sup> 13 kJ/g. Then, for the intervals of steady-state burning, the results from Fig. 3 and eqns (15) and (16) were used to estimate  $\psi$  from  $\dot{Q}_{MEAS}$  (i.e. values of  $\dot{Q}$  determined from the measured values of  $dM/dt$ ) and from  $T$  (estimated to be identical to  $T_{UP, AVE}$ ).

The results of the analyses are summarized in Table 1. In the table,  $\psi_{LOW}$  was estimated from  $c_{LOW, O_2}$  according to  $\psi_{LOW} \approx 0.23 (c_{LOW, O_2}/0.21)$ . Assuming again that  $\psi_{EXT} \approx \psi_{EXT}$  for  $CH_4$ , note that the low  $\psi_{LOW}$  values of experiments 2 and 3, approximately 0.15, indicate that the fire in both cases was close to extinction. The measured values of  $c_{LOW, O_2}$  in these two cases were  $0.137 \pm 0.004$  and  $0.141 \pm 0.002$  for experiments 2 and 3, respectively; these are the lowest  $O_2$  concentrations measured throughout Jansson *et al.*'s<sup>11</sup> test series.

As in their analysis,<sup>11</sup> there are no reported measured values of  $\psi$  to directly confirm the calculated results of Table 1. However, once again the calculated results are plausible, since, as required, they are always less than  $\psi_{LOW}$ .

#### 4 SUMMARY AND CONCLUSIONS

A previously developed model<sup>1</sup> for calculating combined buoyancy- and pressure-driven flow through a shallow, circular, horizontal vent was used to solve the problem of steady burning in a ceiling-vented enclosure. The phenomenon involves an exchange flow at the vent driven by the unstable configuration of relatively cool and dense gas above the vent (the outside air) over elevated-temperature low-density gas below the vent (the heated, product-of-combustion- contaminated air in the enclosure). A solution to the problem, presented in Fig. 3, provides the functional dependence between the energy release rate of the burning fuel, the mass concentration of oxygen in the enclosure, the diameter of the vent and the ratio of inside-to-outside temperature. This indicates that, in general, for specified values of oxygen mass concentration and vent diameter, the

energy release rate from combustion in the enclosure is a maximum for  $T/T_{AMB} = 1.65$ . Also presented in Fig. 3 is the solution for cross-vent pressure difference as a function of inside-to-outside temperature ratio. The Fig. 3 solution was found to be consistent with previously published data involving full-scale ceiling-vented fire scenarios.

### ACKNOWLEDGEMENT

Much of the work presented here was done while the author was a guest of the Fire Research Institute of Japan. The author acknowledges gratefully the gracious hospitality and very useful discussions with the staff of that institution during that visit, and especially those with Dr Tokiyoshi Yamada.

### REFERENCES

1. Cooper, L. Y., Combined buoyancy- and pressure-driven flow through a horizontal, circular vent. *J. Heat Transfer*, **117** (1995) 659–667.
2. Cooper, L. Y., Calculation of the flow through a horizontal ceiling/floor vent. NISTIR 89-4052, National Institute of Standards and Technology, Gaithersburg, MD, 1989.
3. Cooper, L. Y., An algorithm and associated computer subroutine for calculating flow through a horizontal ceiling/floor vent in a zone-type compartment fire model. NISTIR 4402, National Institute of Technology, Gaithersburg, MD, 1990.
4. Morehart, J. H., Zukoski, E. E. & Kubota, T., Characteristics of large diffusion flames burning in a vitiated atmosphere. In *Fire Safety Science—Proc. 3rd Int. Symp.*, ed. G. Cox & B. Langford. Elsevier, New York, 1991, pp. 575–83.
5. Morehart, J. H., Zukoski, E. E. & Kubota, T., Species produced in fires burning in two-layered and homogeneous vitiated environments. California Institute of Technology October 1988, Quarterly Report to National Institute of Standards and Technology, Gaithersburg, MD, August 1990.
6. Press, W. H., Flannery, B. P., Teukolsky, S. A. & Vetterling, W. T., *Numerical Recipes*. Cambridge University Press, Cambridge, MA, 1986, p.258.
7. Epstein, M., Buoyancy-driven exchange flow through small openings in horizontal partitions. *J. Heat Transfer*, **110** (1988) 885–893.
8. Huggett, C., Estimation of rate of heat release by means of oxygen consumption measurements. *Fire Mater.*, **4** (1980) 61–65.
9. Epstein, M., Maximum air flow rate into a roof-vented enclosure fire. *J. Heat Transfer*, **114** (1992) 535–538.
10. Steward, F. R., Morrison, L. & Mehaffey, J., Full-scale fire tests for ship accommodation quarters. *Fire Technol.*, **287** (1992) 31–47.
11. Jansson, R., Onnermark, B. & Halvarsson, K., Fire in a roof-ventilated

- room. FOA Report C 20606-D6, National Defence Research Institute, Stockholm, Sweden, March 1986.
12. Tewardson, A., Generation of heat and chemical compounds in fires. In *SFPE Handbook of Fire Protection Engineering*, ed. P. J. DiNenno, C. L. Beyler, R. L. P. Custer, W. D. Walton & J. M. Watts, Jr. NFPA/SPPE, Quincy, MA, 1988, p. 1-189.

